COMMUNICATION

Furan-Containing Double Tetraoxa[7]helicene and its Radical Cation

Received 00th January 20xx,
Accepted 00th January 20xx

DOI: 10.1039/x0xx00000x

Hao Chang, [a] Haoliang Liu,[b] Evgenia Dmitrieva,[c] Qiang Chen, [d] Ji Ma,[e] Piao He, [a] Pengcai Liu,[f] Alexey A. Popov,[g] Xiao-Yu Cao,[b] Xiao-Ye Wang,[f] Yingping Zou,[a] Akimitsu Narita, [h] Klaus Müllen,[h] Hongjian Peng*[a] and Yunbin Hu*[a]

Abstract: An unprecedented furan-based double oxa[7]helicene 1 was achieved, featuring a stable twisted conformation with π-overlap at both helical ends. The excellent conformational stability allowed for optical resolution of 1, which provided a pair of enantiomers exhibiting pronounced mirror-imaged circular dichroism and circularly polarized luminescence activity. The radical cation of 1 was obtained by chemical oxidation as evidenced by UV-Vis-NIR absorption, electron paramagnetic resonance spectroscopy and *in situ* spectroelectrochemistry. The present work is the starting point for the investigation of open-shell oxahelicenes.

Helicenes are an attractive class of contorted polycyclic aromatics comprising *ortho*-condensed aromatic rings[1]. The inherent helical chirality coupled with nonplanar delocalized π-electron systems endows helicenes with fascinating properties such as circular dichroism (CD)[2], circularly polarized luminescence (CPL)[3], and chiral-induced spin selectivity (CISS)[4], which have already enabled promising applications in chiroptical switching, molecular recognition, chiral photonics, and spintronics[5]. In contrast to conventional monohelicenes, growing interest has recently been attracted by fusing two or more helical moieties to access double or multiple helicenes owing to their extended π-conjugation, increased distortion, and enhanced chiroptical responses[6]. The incorporation of heteroatoms into helicene chains offers new synthetic opportunities to these helical skeletons and holds promise for modulating optoelectronic properties[7]. Oxahelicenes, especially furan-containing helicenes, are expected to possess relatively high HOMO levels and attractive luminescence[8]. Despite significant advances in the synthesis of oxahelicenes by helical elongation[9], as exemplified by the furan-based 1,3,7-trioxa[11]helicene and non-fully aromatic oxa[19]helicene[9c, 9f], little attention has been paid to lateral aromatic annulation[10]. In particular, furan-based double or multiple oxahelicenes with stable chirality have remained elusive

On the other hand, open-shell helicenes with the spin delocalized along the chiral helical framworks are of fundamental interests for emerging magnetochiral properties such as enhanced spin-filtering efficiency[11]. The high intrinsic reactivity of radical species, however, impedes the further development of this field. Up to date, only a few open-shell carbo/thio/azahelicene have been reported,[12] while open-shell oxahelicenes remain unexplored. Herein, we report the facile synthesis of a furan-embedded double oxa[7]helicene **1** via four-fold Suzuki-Miyura coupling and intramolecular Scholl reactions (Scheme 1). Despite two five-membered furan rings contained in each [7]helicene subunit, spatial overlap at both helical ends is sufficient to ensure chiral stability and facilitate optical resolution. In addition, one-electron oxidation of **1** could be expected to provide the corresponding radical cation with considerable spin delocalization through the extended helical π-system.

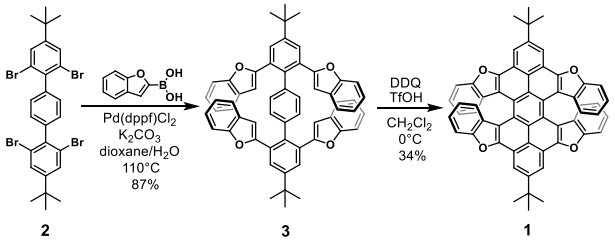

Scheme 1. Synthetic route towards double oxa[7]helicene **1**

Rcently, we demonstrated the synthesis of two double[7]carbohelicene derivatives via intramolecular

[a] College of Chemistry and Chemical Engineering, Central South University, Changsha, Hunan 410083, P. R. China..
[b] Department of Chemistry and Chemical Engineering, Xiamen University, 361005 Xiamen, China..
[c] Center of Spectroelectrochemistry, Leibniz Institute for Solid State and Materials Research, Helmholtzstrasse 20, 01069 Dresden, Germany.
[d] Max Planck Institute for Polymer Research, Ackermannweg 10, 55128 Mainz, Germany
[e] Centre for Advancing Electronics Dresden (cfaed), Faculty of Chemistry and Food Chemistry, Technische Universität Dresden, 01062 Dres-den, Germany
[f] State Key Laboratory of Elemento-Organic Chemistry, College of Chemistry, Nankai University, Weijin Road 94, Tianjin, 300071 China.
[g] Organic and Carbon Nanomaterials Unit, Okinawa Institute of Science and Technology Graduate University
[h] 1919-1 Tancha, Onna-son, Kunigami-gun, Okinawa 904-0495, Japan.
Electronic Supplementary Information (ESI) available: [Experimental procedure and spectral data]. See DOI: 10.1039/x0xx00000x

oxidative cyclodehydrogenation of tailor-made precursors[13]. In this work, we applied a similar procedure to synthesize the double oxa[7]helicene **1** (Scheme 1). First, four benzofuran units were attached to a terphenyl core through a four-fold Suzuki- Miyaura coupling between the commercially available benzofuran-2-boronic acid and tetrabromo terphenyl **2**, affording precursor **3** in 87% yield. Then the intramolecular cyclodehydrogenation of **3** was conducted in dichloromethane /trifilic acid (TfOH) utilizing 2,3-dichloro-5,6-dicyano-1,4-benzoquinone (DDQ) as the oxidant, offering the target double oxa[7]helicene **1** in 34% yield. Double helicene **1** is well soluble in common organic solvents, enabling its structural characterization by ^{1}H- and ^{13}C-NMR spetroscopies in CD_2Cl_2, as well as high-resolution mass spectrometry.

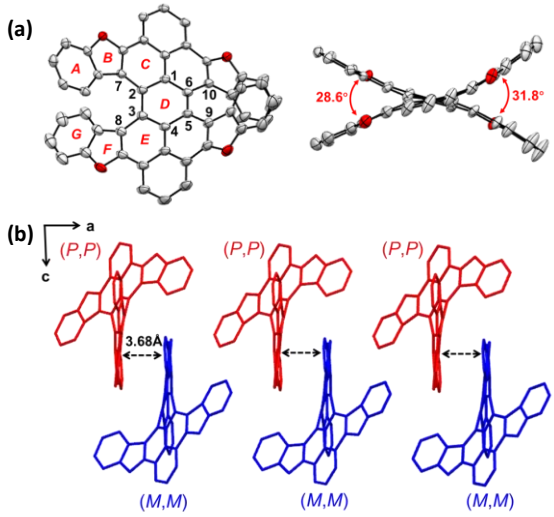

Figure 1. (a) Top and side view of the ORTEP drawing of **1**, providing 50% probability thermal ellipsoids. (b) Packing structure of **1**. (*tert*-butyl chains and hydrogen atoms were omitted for clarification; π-π interactions are indicated with black dotted arrows).

Single-crystal X-ray diffraction analysis further determined the structure of **1**, displaying a cruciform-shaped double helical skeleton (Figure 1a). As expected, the oxa[7]helicene substructure establishes partial overlap between terminal rings A and G. The mean vertical distance between rings A and G is 3.41 Å as defined by the average distance from the centroid of one ring to the plane of the other, reflecting substantial intramolecular interactions. The torsions of the two helicene subunits are determined by dihedral angles of C7-C2-C3-C8 (31.8°) and C10-C6-C5-C9 (28.6°), respectively, which are comparable to those of the previously reported double [7]carbohelicene (30.6° and 28.5°)[13b]. According to density functional theory (DFT) calculation, the optimized strucuture of **1** reveals an equivalent torsion of 30.2° for both helicene subunits (Figure S3). Therefore, the unequal torsions observed in the crystal structure are due to intermolecular packing forces. In the crystal structure (Figure 1b), the enantiomers, (*P*,*P*)-**1** and (*M*,*M*)-**1**, are stacked alternatively along the *a* axis in a remarkable π-dimeric fasion with the π-π distance of 3.68 Å and CH···O short contacts of 2.51 Å (Figure S2).

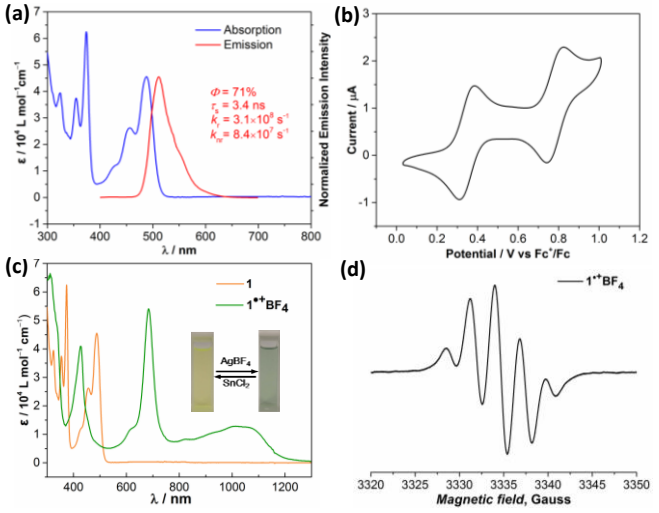

Figure 2. (a) UV-Vis absorption and emission spectra of **1** in DCM. (b) Cyclic Voltammogram of **1**. (c) Absorption spectral change from **1** to $\mathbf{1}^{\bullet+}BF_4$ after addition of excessive $AgBF_4$.Inset: photographs of the solution of **1** and $\mathbf{1}^{\bullet+}BF_4$ in DCM and their interconversion. (b) EPR spectrum of $\mathbf{1}^{\bullet+}BF_4$ produced by oxidation of **1** with $AgBF_4$.

The optical and electrochemical properties of **1** were evaluated in its dichloromethane (DCM) solutions. The absorption spectrum exhibited two major bands at 375 and 488 nm with vibronic fine structures typical for rigid aromatics. The absorption onset at 516 nm corresponds to an optical gap of 2.4 eV (Figure 2a). According to time-dependent (TD)-DFT calculation (Figure S4 and Table S2), the lowest-energy absorption band could be assigned to a large contribution of the HOMO→LUMO transition and a small contribution of the HOMO-1→LUMO+1 transition. Compound **1** displayed strong green fluorescence peaking at 511 nm, with an absolute fluorescence quantum yield (Φ) of 71% and fluorescence lifetime (τ_s) of 3.4 ns. According to the equations $\Phi = k_r \times \tau_s$ and $k_r + k_{nr} = \tau_s^{-1}$, the radiative ($k_r$) and nonradiative ($k_{nr}$) decay rate constants from the singlet excited state were determined (k_r = 2.1 × 10^8 s^{-1}, k_{nr} = 8.4 × 10^7 s^{-1}). Cyclic voltammetry (CV) of **1** exhibited two reversible oxidation waves, with the half-wave potentials at 0.35 and 0.78 V versus Fc/Fc^+ (Figure 2b). The first and second waves are most likely attributed to a one-electron oxidation of **1** to its radical cation and a two-electron oxidation to its dication, respectively.

The isomerization process from (*P*,*P*)-**1** to (*P*,*M*)-**1** through a transition state (TS) was calculated by DFT at the B3LYP/6-311G(d,p) level (Figure 3a). (*P*,*P*)-**1** is estimated to be thermodynamically more stable than (*P*,*M*)-**1** by 9.3 kcal/mol, which explains the absence of (*P*,*M*)-**1** during the synthesis. The calculated isomerization barrier of **1** is 50.5 kcal/mol, suggesting the pronounced conformational stability of double oxa[7]helicene **1**. Accordingly, optical resolution of racemic **1** was performed by chiral high-performance liquid chromatography (HPLC) on a Daicel Chiralpak IE column (Figure S8), providing enantiopure (*P*,*P*)-**1** and (*M*,*M*)-**1**, respectively, as suggested by their mirror-imaged CD spectra (Figure 3b). By

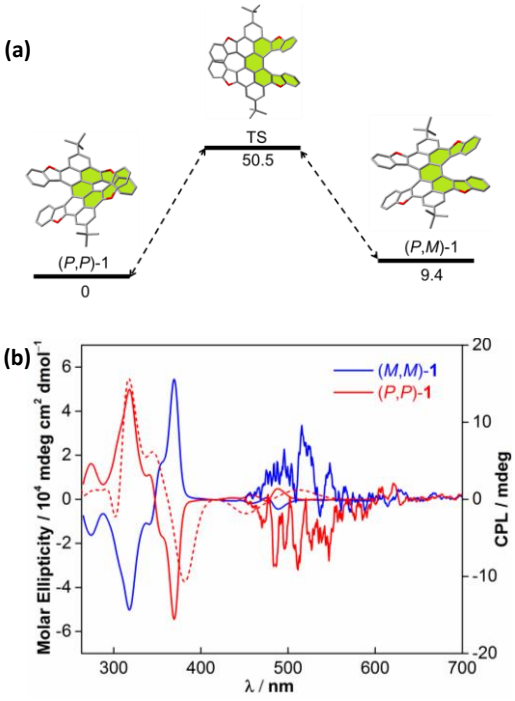

Figure 3. (a) Isomerization process from (*P*,*P*)-**1** to (*P*,*M*)-**1**. The relative Gibbs free energy (unit: kcal mol^{-1}) was calculated at the B3LYP/6-311G(d,p) level. All hydrogen atoms were omitted for clarity. (b) CD and CPL spectra of (*P*,*P*)-**1** and (*M*,*M*)-**1**. The red dotted line shows the CD spectrum for (*P*,*P*)-**1** simulated by TD-DFT at the B3LYP/6-311G(d,p) level.

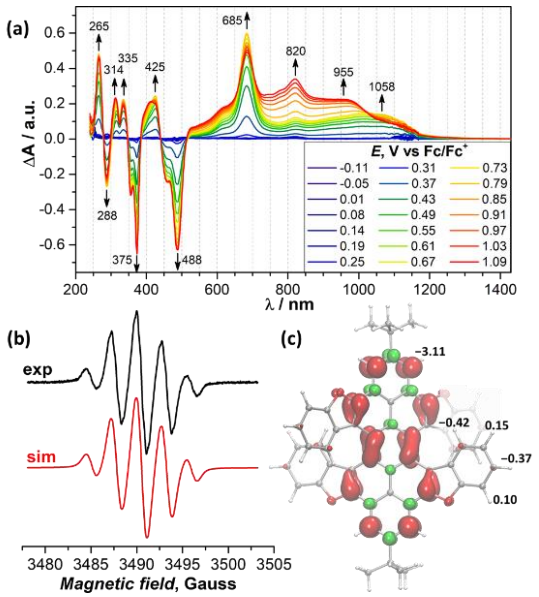

Figure 4. (a) *In situ* UV−Vis−NIR spectra measured during the electrochemical oxidation of **1** in DCM solution (reference spectrum: **1** in electrolyte solution). (b) EPR spectrum of the electrochemically generated radical cation **1**$^{\bullet+}$ (black) and simulated spectrum (red) with fitted parameters (g = 2.0027, *a*(^{1}H): 4×2.73 G, 4×0.32 G, 4×0.31 G, Lorenzian shape). (c) DFT-computed spin density distirbution in the radical cation with averaged ^{1}H hyperfine coupling constants (in Gauss) of the DBP core and terminal benzene rings

comparing the experimental and simulated CD spetra, their absolute configurations were established. In addition, (*P*,*P*)-**1**and (*M*,*M*)-**1** also exhibited CPL activities, as their CPL spectra show mirrored features (Figure 3b), offering a moderate luminescence dissymmetry factor (g_{lum}) of −7.5×10^{-4} at 506 nm for (*P*,*P*)-**1**.

The reversible redox reaction of **1** discussed above reflects the good stabilities of its oxidized species. Therefore, we explored chemical oxidation of **1** to its radical cation by silver(I) tetrafluoroborate ($AgBF_4$) ($E°$ = 0.65 V versus Fc/Fc$^+$ in DCM), which was expected to allow the selective one-electron oxidation. As shown in Figure 2c, upon addition of excessive $AgBF_4$ to a solution of **1** in dry DCM , the light yellow solution turned to green with the appearance of two sharp absorption bands at 425 and 685 nm, as well as a broad near-infrared band in the range of 770–1200 nm. The vanishment of the characteristic bands at 375 and 488 nm indicated the total conversion of **1**. Electron paramagnetic resonance (EPR) measurements of this green solution showed a well-resolved quintet, with apparent ^{1}H-hyperfine coupling constant of a(^{1}H) = 2.75 G and isotropic *g* value of 2.005 (Figure 2d), which could be assigned to the radical cation 1$^{\bullet+}$. In addition, the 1$^{\bullet+}BF_4$ salts was also prepared as greenish black solid by using an excess of oxidant (see supporting information for synthetic details),which could be reversibly reduced back to the neutral compound **1** by adding tin(II) chloride ($SnCl_2$) as evidenced by the recovery of a ^{1}H-NMR spectrum (Figure S17).

To prove the assignment of the chemically-oxidized species to the radical cation, *in situ* EPR/UV−Vis−NIR spectroelectrochemistry of **1** was carried out (Figure 4a). In the first oxidation step, new absorption bands appeared at 425, 685 and 770–1200 nm, whereas the negative peaks developed at 288, 375 and 488 nm. A series of isosbestic points at 275, 300, 324, 346, 385, 437 and 515 nm indicate that only two species, **1** and **1**$^{\bullet+}$, are involved in the process. Appearance of NIR absorptions is accompanied by the growth of the EPR signal with a similar apparent quintet shape as for the chemically-oxidized species (Figure 4b). DFT calculations show that the spin density in the cation is maily distributed over the central dibenzoperylene (DBP) core with minor contributions from the terminal benzene rings. Accoringly, four DBP protons have the highest predicted ^{1}H hyperfine constant (hfc) of −3.11 G (Figure 4c). In the terminal benzene rings, predicted constants are considerably smaller, from 0.10 to −0.42 G. Fitting of the experimental EPR spectrum with the model involving three sets of non-equivalent protons gave the costansts of 2.73, 0.32, and 0.31 G, in good agreement with DFT predictions. Overall, the hfc constant other than for DBP protons are not sufficiently large to be clearly resolved in the spectrum. The perfect correspondence of the EPR and UV-Vis-NIR spectra of electrochemically and chemically oxidized **1** unambiguously confirms reasonable stability of **1**$^{\bullet+}$. In the second oxidation step, the absorption bands at 820 and 955 nm becomes dominant accompanied by the decreasing EPR signal (Figure S7). This pointed toward the formation of diamagnetic species, namely dication.

In summary, we present the synthesis of an unprecedented furan-based double oxa[7]helicene **1** along with its characterization. The crystallography analysis unambiguously disclose the double helical structure of **1** with high distortion. Our work demonstrates the efficiency of intramolecular cyclodehydrogenation of furan moieties, and thus holds promise for further furan-based double or multiple helicenes. The reversible redox property of **1** as suggested by CV allowed us to prepare stable radical cation $\mathbf{1}^{\bullet+}$ by chemical oxidation, which was characterized by in-situ UV-Vis-NIR and EPR spectroelectrochemistry. Moreover, the pair of enantiomers, (*P*,*P*)-**1** and (*M*,*M*)-**1**, were successfully separated using chiral HPLC, allowing to study their chiroptical properties by CD and CPL spectroscopy. These intriguing properties of **1** prompt further studies into chiral photonics and spintronics

Conflicts of interest

There are no conflicts to declare.

Acknowledgement

This work was financially supported by the National Natural Science Foundation of China (No. 21901257) and Innovation-Driven Project of Central South University (No. 502501009). X.-Y. W. thanks the financial support from the National Natural Science Foundation of China (No. 21901128).

Notes and references

1 (a) M. Gingras, *Chem. Soc. Rev.*, 2013, **42**, 1051-1095; (b) M. Gingras, *Chem. Soc. Rev.*, 2013, **42**, 968-1006; (c) M. Gingras, G. Felix and R. Peresutti, *Chem. Soc. Rev.*, 2013, **42**, 1007-1050; (d) Y. Shen and C.-F. Chen, *Chem. Rev.*, 2012, **112**, 1463−1535.

2 N. Berova, L. Di Bari and G. Pescitelli, *Chem. Soc. Rev*. 2007, **36**, 914-931.

3 J. Han, S. Guo, H. Lu, S. Liu, Q. Zhao and W. Huang, *Adv. Opt. Mater.*, 2018, **6**, 1800538.

4 R. Naaman and D. H. Waldeck, *J. Phys. Chem. Lett.*, 2012, **3**, 2178-2187.

5 (a) J. M. Matxain, J. M. Ugalde, V. Mujica, S. I. Allec, B. M. Wong and D. Casanova, *Chemphotochem*, 2019, **3**, 770-777; (b) T. R. Schulte, J. J. Holstein and G. H. Clever, *Angew. Chem. In. Ed.*, 2019, **58**, 5562-5566; (c) J. R. Brandt, X. Wang, Y. Yang, A. J. Campbell and M. J. Fuchter, *J. Am. Chem. Soc.*, 2016, **138**, 9743-9746; (d) V. Kiran, S. P. Mathew, S. R. Cohen, I. H. Delgado, J. Lacour and R. Naaman, *Adv. Mater.*, 2016, **28**, 1957-1962; (e) D. Schweinfurth, M. Zalibera, M. Kathan, C. Shen, M. Mazzolini, N. Trapp, J. Crassous, G. Gescheidt and F. Diederich, *J. Am. Chem. Soc.*, 2014, **136**, 13045-13052; (f) T.-R. Pan, A.-M. Guo and Q.-F. Sun, *Phys. Rev. B*, 2016, **94**, 235448; (g) L. Pospíšil, L. Bednárová, P. Štěpánek, P. Slavíček, J. Vávra, M. Hromadová, H. Dlouhá, J. Tarábek and F. Teplý, *J. Am. Chem. Soc.*, 2014, **136**, 10826-10829; (h) O. Kel, A. Fürstenberg, N. Mehanna, C. Nicolas, B. Laleu, M. Hammarson, B. Albinsson, J. Lacour and E. Vauthey, *Chem. Eur. J.*, 2013, **19**, 7173-7180; (i) Y. Yang, R. C. da Costa, M. J. Fuchter and A. J. Campbell, *Nat. Photonics*, 2013, **7**, 634−638; (j) E. Anger, M. Srebro, N. Vanthuyne, L. Toupet, S. Rigaut, C. Roussel, J. Autschbach, J. Crassous and R. Réau, *J. Am. Chem. Soc.*, 2012, **134**, 15628-15631.

6 (a) W.-B. Lin, M. Li, L. Fang and C.-F. Chen, *Chin. Chem. Lett.*, 2018, **29**, 40-46; (b) C. Li, Y. Yang and Q. Miao, *Chem. Asian J.*, 2018, **13**, 884−894.

7 K. Dhbaibi, L. Favereau and J. Crassous, *Chem. Rev.*, 2019, **119**, 8846-8953.

8 (a) K. Nakanishi, T. Sasamori, K. Kuramochi, N. Tokitoh, T. Kawabata and K. Tsubaki, *J. Org. Chem.*, 2014, **79**, 2625-2631; (b) M. S. Sundar and A. V. Bedekar, *Org. Lett.*, 2015, **17**, 5808-5811; (c) T. Matsuno, Y. Koyama, S. Hiroto, J. Kumar, T. Kawai and H. Shinokubo, *Chem. Commun.*, 2015, **51**, 4607-4610.

9 (a) I. G. Stará and I. Starý, *Acc. Chem. Res.*, 2020, **53**, 144-158; (b) J. Nejedlý, M. Šámal, J. Rybáček, I. G. Sánchez, V. Houska, T. Warzecha, J. Vacek, L. Sieger, M. Buděšínský, L. Bednárová, P. Fiedler, I. Císařová, I. Starý and I. G. Stará, *J. Org. Chem.*, 2020, **85**, 248-276; (c) J. Nejedlý, M. Šámal, J. Rybáček, M. Tobrmanová, F. Szydlo, C. Coudret, M. Neumeier, J. Vacek, J. V. Chocholoušová, M. Buděšínský, D. Šaman, L. Bednárová, L. Sieger, I. G. Stará and I. Starý, *Angew. Chem. In. Ed.*, 2017, **56**, 5839-5843; (d) M. Shahabuddin, K. Ohgoshi, S. Hossain, T. Kimura and M. Karikomi, *Tetrahedron Lett.*, 2017, **58**, 3704-3707; (e) M. Sako, Y. Takeuchi, T. Tsujihara, J. Kodera, T. Kawano, S. Takizawa and H. Sasai, *J. Am. Chem. Soc.*, 2016, **138**, 11481-11484; (f) M. S. Sundar and B. Ashutosh, *Org. Lett.*, 2016, **18**, 1710-1710; (g) M. Salim, A. Akutsu, T. Kimura, M. Minabe and M. Karikomi, *Tetrahedron Lett.*, 2011, **52**, 4518−4520; (h) K. Nakano, Y. Hidehira, K. Takahashi, T. Hiyama and K. Nozaki, *Angew. Chem. In. Ed.*, 2005, **44**, 7136-7138; (i) J. Areephong, N. Ruangsupapichart and T. Thongpanchang, *Tetrahedron Lett.*, 2004, **45**, 3067-3070; (j) J. Eskildsen, F. C. Krebs, A. Faldt, P. Sommer-Larsen and K. Bechgaard, *J. Org. Chem.*, 2001, **66**, 200-205; (k) M. Shahabuddin, M. Salim, M. Tomura, T. Kimura and M. Karikomi, *Tetrahedron Lett.*, 2016, **57**, 5902-5906.

10 D. Reger, P. Haines, F. W. Heinemann, D. M. Guldi and N. Jux, *Angew. Chem. In. Ed.*, 2018, **57**, 5938−5942.

11 (a) R. Naaman, Y. Paltiel and D. H. Waldeck, *Nat. Rev. Chem.*, 2019, **3**, 250-260; (b) R. Sessoli, M.-E. Boulon, A. Caneschi, M. Mannini, L. Poggini, F. Wilhelm and A. Rogalev, *Nat. Phys.*, 2015, **11**, 69-74; (c) G. L. J. A. Rikken and N. Avarvari, *Phys. Rev. B*, 2019, **99**, 245153; (d) F. Pop, P. Auban-Senzier, E. Canadell, G. L. J. A. Rikken and N. Avarvari, *Nat. Commun.*, 2014, **5**, 3757; (e) G. L. J. A. Rikken, J. Fölling and P. Wyder, *Phys. Rev. Lett.*, 2001, **87**, 236602.

12 (a) P. Ravat, P. Ribar, M. Rickhaus, D. Häussinger, M. Neuburger and M. Juríček, *J. Org. Chem.*, 2016, **81**, 12303-12317; (b) J. K. Zak, M. Miyasaka, S. Rajca, M. Lapkowski and A. Rajca, *J. Am. Chem. Soc.*, 2010, **132**, 3246-3247; (c) Y. Wang, H. Zhang, M. Pink, A. Olankitwanit, S. Rajca and A. Rajca, *J. Am. Chem. Soc.*, 2016, **138**, 7298-7304; (d) C. Shu, H. Zhang, A. Olankitwanit, S. Rajca and A. Rajca, *J. Am. Chem. Soc.*, 2019, **141**, 17287-17294.

13 (a) Y. Hu, G. M. Paterno, X.-Y. Wang, X.-C. Wang, M. Guizzardi, Q. Chen, D. Schollmeyer, X.-Y. Cao, G. Cerullo, F. Scotognella, K. Müllen and A. Narita, *J. Am. Chem. Soc.*, 2019, **141**, 12797-12803; (b) Y. Hu, X.-Y. Wang, P.-X. Peng, X.-C. Wang, X.-Y. Cao, X. Feng, K. Müllen and A. Narita, *Angew. Chem. In. Ed.*, 2017, **56**, 3374−3378.

